Journal of Thoracic Oncology Publish Ahead of Print

DOI: 10.1097/JTO.0000000000000364

Increase in activated Treg in TIL in lung cancer and in vitro depletion of Treg by ADCC using an anti-human CCR4 mAb (KM2760)

Koji Kurose, M.D.[1], Yoshihiro Ohue, M.D., Ph.D.[1], Eiichi Sato, M.D., Ph.D.[2], Akira Yamauchi, M.D., Ph.D.[3], Shingo Eikawa, Ph.D.[4], Midori Isobe, Ph.D.[1], Yumi Nishio, M.S.[1], Akiko Uenaka, Ph.D.[5], Mikio Oka, M.D., Ph.D.[1], and Eiichi Nakayama, M.D., Ph.D.[5]

Departments of [1]Respiratory Medicine and [3]Biochemistry, Kawasaki Medical School, Kurashiki, Japan; [2]Department of Pathology, Tokyo Medical University, Tokyo, Japan; [4]Department of Immunology, Okayama University Graduate School of Medicine, Dentistry and Pharmaceutical Sciences, Okayama, Japan; [5]Faculty of Health and Welfare, Kawasaki University of Medical Welfare, Kurashiki, Japan.

Correspondence: Eiichi Nakayama, M.D., Ph.D., Faculty of Health and Welfare, Kawasaki University of Medical Welfare, 288 Matsushima, Kurashiki, Okayama 701-0193, Japan.

Phone: +81-86-462-1111 ext. 54954

Fax: +81-86-464-1109

E-mail: nakayama@mw.kawasaki-m.ac.jp

Grant support

This study was supported by the P-DIRECT, Ministry of Education, Culture, Sports, Science and Technology of Japan to E. Nakayama, by a grant from the Ministry of Health Labour and Welfare of Japan to E. Nakayama and M. Oka, by JSPS KAKENHI (23591169 to M. Oka and 25430161 to E. Nakayama), by a Research Project Grant from Kawasaki Medical School to K. Kurose, by a grant from Kawasaki University of Medical Welfare to E. Nakayama and by a grant from Kyowa Hakko Kirin to E. Nakayama.

Disclosure of potential conflicts of interest

This work was funded by Kyowa Hakko Kirin.

Abstract

Introduction: Tregs infiltrate tumors and inhibit immune responses against them.

Methods: We investigated subpopulations of Foxp3$^+$ CD4 T cells previously defined by Miyara et al. (Immunity 30, 899-911, 2009) in PBMCs and TILs in lung cancer. We also showed that Tregs in healthy donors that express CCR4 could be efficiently eliminated in vitro by co-treatment with anti-human (h) CCR4 mAb (KM2760) and NK cells.

Results: In lung cancer, the number of activated/effector Tregs and non Tregs, but not resting/naïve Tregs, was increased in TILs compared to the number of those cells in PBMCs. The non Treg population contained Th2 and Th17. CCR4 expression on activated/effector Tregs and non Tregs in TILs was down-regulated compared to that on those cells in PBMCs. Chemokinetic migration of CD25$^+$ CD4 T cells containing the Treg population sorted from the PBMCs of healthy donors to CCL22/MDC was abrogated by pretreatment with anti-hCCR4 mAb (KM2760). The inhibitory activity of CD25$^+$ CD127$^{dim/-}$ CD4 Tregs on the proliferative response of CD4 and CD8 T cells stimulated with anti-CD3/CD28 coated beads was abrogated by adding an anti-hCCR4 mAb (KM2760) and CD56$^+$ NK cells to the culture.

Conclusions: The findings suggested the CCR4 on activated/effector Tregs and non Tregs was functionally involved in the chemokinetic migration and accumulation of those cells to the tumor site. In vitro findings of efficient elimination of Tregs may give the basis for implementation of a clinical trial to investigate Treg depletion by administration of an anti-hCCR4 mAb to solid cancer patients.

Key Words: Lung cancer, Tregs, CCR4, anti-hCCR4 mAb, Treg depletion

Introduction

Infiltration of Tregs to local tumor sites has been shown in various murine and human tumors.[1] Tregs inhibit immune responses against tumors and also diminish the immunotherapeutic effects which activate host immune responses.[2, 3] The CD8 T cells to Tregs ratio correlated with a favorable prognosis in some human cancers.[4, 5] Tregs appeared to inhibit the priming of CD8 and also CD4 T cells by preventing the maturation of dendritic cells (DCs) in tumor-draining lymph nodes.[6] Depletion of Tregs facilitated the induction of anti-tumor responses.[7] Two main populations of $Foxp3^+$ Tregs have been identified: a "naturally occurring" (n) Treg which differentiates within the thymus during T cell ontogenesis and an "induced" (i) Treg which develops in the periphery from conventional CD4 T cells.[8] Conversion of CD4 T cells into iTregs occurs via various mechanisms involving the exposure to TGFβ and other inhibitory cytokines, IL-6 or IL-10, and the interaction with DCs.[9]

The accumulation of Tregs is mainly due to chemokine gradients. Chemokine receptors such as CCR4, CCR5, CCR6, CCR7 and CCR8 are responsible for Treg migration to tumor tissues, and also inflammatory sites and lymph nodes in response to various CC chemokines.[10] Of those, Tregs preferentially express CCR4 as compared to conventional T cells.[11] Moreover, CCR4-expressing Tregs represent active Tregs with strong inhibitory activity. The involvement of CCR4 and CCR4-associated chemokines, CCL17/TARC and CCL22/MDC, in Treg migration have been documented.[12, 13] Tumor cells or intra-tumor myeloid cells produce CCL17/TARC and CCL 22/MDC.

Foxp3 is a key transcription factor for CD4 Tregs.[14] Miyara et al. reported that human $Foxp3^+$ CD4 T cells were composed of three functionally and phenotypically distinct subpopulations.[15] $CD45RA^+$ Foxp3 lo resting/naïve Tregs and $CD45RA^-$ Foxp3 hi

activated/effector Tregs were suppressive, while a CD45RA$^-$ Foxp3 lo population was made up of non-suppressive, non Tregs.

In this study, we investigated the frequency of these three subpopulations in PBMCs and TILs in lung cancer, and showed the accumulation of activated Tregs and also non Tregs in the tumor microenvironment. We also examined the expression of CCR4 on these subpopulations and of chemokines in monocytes to clarify the mechanisms of Treg accumulation in lung cancer. Furthermore, we showed efficient Treg depletion by an anti-hCCR4 mAb (KM2760) and suggested its potential use in solid cancer patients.

Materials and Methods

Patients and clinical samples

For preparation of a lung cancer tissue microarray (TMA), 384 specimens including 204 adenocarcinomas, 114 squamous cell carcinomas, 4 large cell carcinomas, 16 small cell carcinomas, 8 adenosquamous cell carcinomas and 4 others, and 34 metastatic tumors were used. Tumors were surgically removed from 384 patients who visited the Toyama Medical School Hospital from December 1979 to May 2006. Some patients received chemotherapy or radiation therapy before surgery. For Treg analysis, PBMCs and tumor specimens were obtained from 20 patients with lung cancer who underwent surgery at Kawasaki Medical School Hospital from March 2012 to March 2014. For T cell migration and proliferation analysis, PBMCs from 3 healthy donors were used. Peripheral blood or tumor specimens were obtained from healthy donors or patients after obtaining informed consent. These studies were approved by the ethics committee of Toyama University Hospital (IRB no. 19-12) and Kawasaki Medical School Hospital (IRB no. 603-6) and conducted in accordance with the Declaration of Helsinki.

Immunohistochemistry (IHC)

The tissue microarray (TMA) was prepared for 2 tumor nests in each sample punched out (core size, 0.6 mm) from formalin-fixed paraffin-embedded tumor tissues. For staining, a 4 μm thick section on a slide was used. To stain CCR4, a POTELIGEO ®TEST IHC (Kyowa Medex, Tokyo) was used. Briefly, after being deparaffinized, a tissue section was put in an oven for antigen retrieval for 40 min at 98℃. Endogenous peroxidase was blocked by adding 1N HCl for 10 min. Mouse anti-hCCR4 mAb (KM2160) (1:200) was then added and incubated for 30 min. As a second antibody, a peroxidase-conjugated goat anti-mouse IgG (1:1000) was added and incubated for 30 min. For staining CD4 and Foxp3, a rabbit anti-hCD4 mAb (clone EPR6855; abcam) (1:100) and a mouse anti-hFoxp3 mAb (clone 236A/E7; abcam) (1:100), respectively, were added and incubated for 30 min. For doublestaining of CCR4 and CD4, a mouse/rabbit multiplex detection system (Diagnostic Biosystems, MP-001) was used. For staining of CCL17/TARC, goat anti-hCCL17/TARC (1:40) was used and incubated for 60 min. Simple stain MAX-PO (G) (Nichirei, 414161) was used as a second antibody and incubated overnight. For staining of CCL22/MDC, a mouse anti-hCCL22/MDC mAb (clone 57226; R&D Systems) (1:50) was used and incubated overnight. For staining of CD163, a mouse anti-hCD163 mAb (clone 10D6; abcam) (1:1) was used and incubated for 30 min. As a second antibody, Envision Dual Link reagent (Dako) was used and incubated for 30 min. Counterstaining was done with hematoxylin.

IHC scoring of TMA

Interstitial cells and tumor cells were scored separately by the grade of distribution and intensity.[16] For grading distribution, 0 for 0%; 1 for 1-50%; 2 for 51-100% were used.

For grading intensity, 0 for no staining; 1 for weak staining; 2 for moderate staining and 3 for marked staining were used. The mean of the sum of distribution and intensity scores from two distinct tumor TMA histospots was used as the definitive IHC score. Scores exceeding 2 ($\geq$ 2.5) were defined positive. Scoring was performed by a pathologist.

Isolation of TILs

TILs were freshly isolated from lung cancer tissues using a Medimachine (BioLab, Osaka, Japan). Briefly, the tumor tissue was minced into pieces (<1 mm^3) and placed on a stainless steel screen with approximately 100 hexagonal holes, each surrounded by six microblades, in a sterile Medicon polyethylene chamber (BioLab) in 1ml medium. A rotating screen brings the tissue into contact with the blades and it is homogenized. A Medicon with 50 µm separator screens was used. The procedure was repeated 3 times for 60 sec at a constant speed of 100 rpm. Cells were collected after filtration using filters with a 50 µm pore size and then TILs were isolated.

Flow cytometry

PBMCs and TILs were isolated by density gradient centrifugation using a Histo-Paque 1077 (Sigma-Aldrich, St. Louis, MO). Freshly isolated PBMCs or TILs were incubated with a mAb for 20 min at 4℃. The following mAbs were used: Anti-hCD3-V450 (clone UCHT1; BD Horizon™, BD Bioscience, San Jose, CA, USA), anti-hCD4-V500 (clone RPA-T4; BD Horizon™), anti-hCD8-APC (clone RPA-T8; BD Pharmingen™), anti-hCCR4-PerCP/Cy5.5 (clone 1G1; BD Pharmingen™), anti-hFoxp3-Alexa Fluor 488 (clone 259D/C7; BD Pharmingen™), and anti-hCD45RA- APC/H7 (clone HI100; BD Pharmingen™). Intracellular Foxp3 staining was performed using a Human Foxp3 buffer set (BD Pharmingen™) according to the manufacturer's instructions. With each

sample, an isotype-matched control Ab was used to determine the positive and negative cell populations. Analysis was done by FACS Canto II.

CFSE labeling

A CFSE stock (10 mM in DMSO: Molecular Probes, Eugene, OR) stored at -30℃ was thawed and diluted in PBS. The CD4 or CD8 T cells (5 x 10^6 cells/ml) in 0.1% BSA PBS were incubated with 10 μM CFSE for 10 min at 37℃, diluted by five volumes of cold 0.1% BSA PBS, and kept on ice for 5 min. Cells were washed three times and used for experiments.

Cell migration assay

The cell migration was examined using EZ-TAXIScan™ (Effector Cell Institute, Tokyo Japan) apparatus.[17, 18] Two compartments of a cell migration assay chamber in etched silicon were connected by a 4 μm deep micro-channel on a flat glass plate in the chamber. A glass coverslip was placed onto the glass plates. A reproducible chemoattractant gradient was formed in the micro-channel without medium flow. The holder was filled with AIM V® (Invitrogen) supplemented with 2.5% heat-inactivated pooled human serum and maintained at 37℃. $CD25^+$ CD4 T cells (1 x 10^5 cells in 1 μl) sorted from PBMCs which were left untreated or treated with anti-hCCR4 mAb (KM2760) (provided by Kyowa Hakko Kirin, Tokyo, Japan) using FACS Aria were injected into one compartment and 1 μl of CCL22/MDC (500 μg/ml, R&D Systems) solution into the other compartment. The migration of each cell in the channel was traced at time-lapse intervals using a CCD camera and recorded every 1 min for 60 min. The cells that crossed a fixed gate were counted using a TAXIScan Analyzer (Effector Cell Institute).

To examine blocking activity of anti-hCCR4 mAb (KM2760) on migration, 24-well Transwell chemotaxis plates (4 μm pore size; Corning Costar) were used. CD4 T cells ($1x10^5$) were placed in the upper chamber of a Transwell plate. Various concentrations of anti-hCCR4 mAb (KM2760) were added to both the upper and lower chambers. Then, CCL22/MDC (100 ng/ml) was added to the lower chamber and incubated for 4 hrs at 37℃. After incubation, all cells in the lower chamber were collected and the number of cells was counted with a FACS Canto II.

Proliferation assay

To obtain Tregs, a regulatory T cell isolation kit II (Miltenyi Biotec, Bergisch Gladbach, Germany) was used. $CD127^{dim/-}$ CD4 T cells were indirectly purified from PBMCs of healthy donors using biotin-conjugated antibodies against CD8, CD19, CD123 and CD127 with anti-biotin antibody-coated magnetic beads. $CD25^+$ $CD127^{dim/-}$ CD4 Tregs were then purified and $CD25^-$ $CD127^{dim/-}$ CD4 T cells were used as control cells. $CD56^+$ NK cells, and CD4 and CD8 T cells were purified from PBMCs also using antibody-coated magnetic beads (Miltenyi Biotec). Tregs (1×10^4) and $CD56^+$ NK cells (1×10^4) were incubated overnight with or without anti-hCCR4 mAb (KM2760) at a concentration of 10 μg/ml in 96-well culture plates. The cells in the plates were washed three times and anti-hCD3/28 beads (Dynabeads® Human T-Activator CD3/CD28, Invitrogen) were added to the culture and incubated for 8 hrs for suppressor cell stimulation. CFSE-labeled responder cells (1×10^4 /well) were then added and stimulated by anti-CD3/28 beads. After 24 hrs, anti-CD3/28 beads were removed and the cells were kept cultured for another 3-4 days. After culture, the cells were harvested and CFSE dilution was analyzed with a FACS Canto II. The medium used was AIM V® (Invitrogen) supplemented with 5% heat-inactivated pooled human serum, 2 mM L-glutamine, 100 IU/ml penicillin, and 100 μg/ml streptomycin.

Results

Subpopulations of Foxp3$^+$ CD4 T cells and expression of CCR4 on those cells in PBMCs and TILs from lung cancer patients

Subpopulations of Foxp3$^+$ CD4 T cells and expression of CCR4 on those cells in PBMCs and TILs from lung cancer patients were analyzed. The characteristics of 20 patients investigated are shown in Table 1. As shown in Fig. 1, Foxp3$^+$ CD4 T cells were classified as three subpopulations: CD45RA$^+$ Foxp3^{lo} resting/naïve Tregs (Fr 1), CD45RA$^-$ Foxp3^{hi} activated/effector Tregs (Fr 2) and CD45RA$^-$ Foxp3^{lo} non Tregs (Fr 3), as described by Miyara et al. .[15] The mean ratios of resting/naïve and activated/effector Tregs, and non Tregs in CD4 T cells in PBMCs from 20 lung cancer patients were 0.6%, 1.6% and 4.1%, respectively. On the other hand, the mean ratios of resting/naïve and activated/effector Tregs, and non Tregs in CD4 T cells in TILs were 0.5%, 9.9% and 9.8%, respectively. The ratios of activated/effector Tregs and non Tregs, but not resting/naïve Tregs, in CD4 T cells in TILs were higher than those in PBMCs.

The CCR4 expression on those populations was then determined. The mean ratios of CCR4$^+$ cells in resting/naïve and activated/effector Tregs, and non Tregs in PBMCs were 13.0%, 88.7% and 65.6%, respectively. On the other hand, the mean ratios of CCR4$^+$ cells in activated/effector Tregs and non Tregs in TILs were 34.6% and 28.5%, respectively. Insufficient resting/naïve Tregs were available for the analysis in TILs. The ratios of CCR4$^+$ cells in activated/effector Tregs and non Tregs in TILs were lower than those in PBMCs.

Detection of CCR4- and CCL22/MDC-expressing cells in lung cancer by IHC using a tissue microarray (TMA)

CCR4, CCL17/TARC and CCL22/MDC-expressing cells in lung cancer were analyzed

by IHC using TMA. For evaluation, the staining score was determined by the sum of scores of distribution and intensity (see Materials and Methods). Two TMA spots were examined in each sample and the mean score was calculated for the definitive score. A definitive score exceeding 2 (≥ 2.5) was defined as positive. As shown in Fig. 2A and B, CCR4-expressing stroma infiltrating lymphocytes were detected in 78 (20.3%) of 384 samples and CCR4-expressing tumor cells were detected in only one (0.3%). CCL17/TARC-expressing stroma infiltrating monocytes were detected in 5 (1.3%) of 384 samples and CCL17/TARC-expressing tumor cells were detected in 2 (0.5%). CCL22/MDC-expressing stroma infiltrating monocytes were detected in 117 (30.5%) of 384 samples and CCL22/MDC-expressing tumor cells were detected in none. As shown in Fig. 3A, CCR4-stained lymphocytes were mostly CD4 and some of those cells were also positive for Foxp3. As shown in Fig. 3B, some CCL22/MDC-expressing cells were likely to be CD163-positive M2 macrophages. CCR4 expression was correlated with CCL22/MDC (Fig. 3C).

By ELISA using plasma and malignant pleural effusion, we detected a significant amount of CCL17/TARC in one patient and CCL22/MDC in several patients out of a total 17 lung cancer patients in a separate analysis (data not shown). Predominance of CCL22/MDC compared to CCL17/TARC in lung cancer was consistent with the IHC results.

Efficient migration of a CCR4$^+$CD25$^+$ CD4 T cell population in PBMCs to the CCL22/MDC gradient and elimination of migrating cells by adding an anti-hCCR4 mAb (KM2760) to the culture

Anti-human (h) CCR4 mAb (KM2760) is a defucosylated antibody developed by the Potelligent ® technology and it has been shown to exert ADCC against CCR4-expressing cells by using NK cells as effector cells.[19] We examined the

migration of $CD25^+$ CD4 T cells sorted from PBMCs which were left untreated or treated with anti-hCCR4 mAb (KM2760) to the CCL22/MDC gradient using EZ-TAXIScan apparatus. Expression of CCR4 on sorted cells was confirmed with a FACS Canto II (data not shown). As positive and negative controls for migration, $CCR4^+$ CD4 T cells and $CCR4^-$ CD4 T cells sorted from anti-hCCR4 mAb (1G1) (with no ADCC activity) and anti-hCD4 mAb-treated PBMCs were used. As shown in Fig. 4, efficient migration to the CCL22/MDC gradient was observed in a $CD25^+$ CD4 T cell population sorted from anti-hCCR4 mAb (KM2760)-untreated PBMCs. Migrating cells were markedly diminished in a $CD25^+$ CD4 T cell population sorted from anti-hCCR4 mAb (KM2760)-treated PBMCs.

We further examined whether an anti-hCCR4 mAb (KM2760) could directly block the migration of CD4 T cells to the CCL22/MDC gradient without NK cells using Transwell plates. As shown in Fig. 4C, anti-hCCR4 mAb (KM2760) had no blocking effect on migration of CD4 T cells or any Treg population in a range of antibody concentrations.

Inhibition of CD3/CD28-mediated proliferative response of CD4 and CD8 T cells by $CD25^+$ CD4 Tregs and abrogation of inhibition by treatment with an anti-hCCR4 mAb (KM2760)

We then examined inhibition of CD4 and CD8 T cell proliferation by Tregs and abrogation of inhibition by the treatment of Tregs with an anti-hCCR4 mAb (KM2760). $CD127^{dim/-}$ CD4 T cells were indirectly purified from PBMCs of healthy donors using biotin-conjugated antibodies against CD8, CD19, CD123 and CD127 with anti-biotin antibody-coated magnetic beads. $CD25^+$ $CD127^{dim/-}$ CD4 Tregs were then purified and $CD25^-$ $CD127^{dim/-}$ CD4 T cells were used as control cells. $CD56^+$ NK cells, and CD4 and CD8 T cells were purified from PBMCs also using antibody-coated magnetic beads. Tregs (1×10^4) and $CD56^+$ NK cells (1×10^4) were incubated overnight with or

without anti-hCCR4 mAb (KM2760) at a concentration of 10 μg/ml in 96-well culture plates. After washing the cells in the plates, anti-CD3/CD28 beads were added. The CFSE-labeled responder CD4 and CD8 T cells were then added and proliferation was determined after 5-6 days. As shown in Fig. 5, proliferation of either CD4 or CD8 T cells stimulated by anti-CD3/CD28 beads was inhibited by culturing with $CD25^+$ $CD127^{dim/-}$ CD4 Tregs and $CD56^+$ NK cells without anti-hCCR4 mAb (KM2760). The inhibition was abrogated in the culture with an anti-hCCR4 mAb (KM2760).

Discussion

$Foxp3^+$ CD4 T cells were composed of three distinct populations and classified according to the expression of CD45RA and Foxp3 on those cells.[15] In this study, we showed that the ratios of activated/effector Tregs and non Tregs in $Foxp3^+$ CD4 T cells were higher in TILs obtained from surgically removed specimens than those in PBMCs in lung cancer patients. The findings suggested that the activated/effector Tregs and also non Tregs appeared to accumulate in the tumor from PBMCs. No increase in resting/naïve Tregs in TILs suggests conversion from resting/naïve Tregs to activated/effector Tregs in the tumor as described previously.[15, 20] The non Treg population contains Th2 and Th17 that could be involved in effector mechanisms in tumors.[1, 15] In our analysis of TILs from 11 lung cancer patients, $CD45RA^-$ Foxp3 lo, a non Treg population contained CRTH2 (CD294)-positive Th2 cells (approximately 9%) and CCR6-positive Th17 cells (approximately 14%), although the rest of cells were not clearly analyzed. Miyara et al. reported detection of transcription factor RORC and secretion of IL-17, and also secretion of IFNγ in stimulation with PMA/ionomycin with the cells in the population.[15] Thus, a small fraction of Th2, Th17 or IFNγ-producing cells was detected in the $CD45RA^-$ Foxp3 low positive, non Treg fraction (Fr 3),

although the majority of those cells were Foxp3-negative cells.

With regard to Th17 cells, it has recently been shown that the frequency of these cells secreting IL-17 was increased in patients with different types of tumors[21], including lung cancer.[22] The density of intratumoral IL-17-positive cells in primary human NSCLC was inversely correlated with patient outcome and correlated with the smoking status of the patients.[23]

We also showed that CCR4 expression on activated/effector Tregs and also non Tregs in TILs was down-regulated compared to that on those cells in PBMCs. It was noticed that chemokine receptors, including CCR4, were down-regulated quickly after interaction with the respective chemokines.[24] These findings suggested that CCR4 was functionally involved with chemotactic migration and accumulation of activated/effector Tregs and non Tregs to the tumor sites.

We demonstrated that CCR4-expressing lymphocytes infiltrated in tumor tissue and some of them were likely $Foxp3^+$ CD4 T cells as judged by IHC using TMA. CCR4-stained lymphocytes were detected in only 20% of the tumor tissues of 384 samples examined, while flow cytometric analysis showed that activated/effector Tregs were detected in TILs from most of the 20 lung cancer patients we investigated. Detection of CCR4-expressing cells at a low frequency in TMA appeared to be due to the limited area of tumor tissue prepared for TMA and/or low sensitivity of IHC.[16] Anti-hCCR4 mAb (KM2760) is a defucosylated chimeric mAb produced by Potelligent ® technology and has been shown to have more than 100 times stronger ADCC activity than the original antibody.[25] Leukemic cells in adult T cell leukemia (ATL) express CCR4 on their surfaces and cytotoxicity of anti-hCCR4 mAb (KM2760) to those cells has been demonstrated.[26] Yamamoto et al. reported that administration of even a small dose (0.1 mg/kg) of humanized anti-hCCR4 mAb (KW-0761) efficiently eliminated leukemia cells in the peripheral blood in adult T cell leukemia (ATL) patients

in clinical trials.[27] In this study, we showed that activated/effector Tregs also express CCR4 on their surface and that those cells could be efficiently eliminated in vitro by treatment with an anti-hCCR4 mAb (KM2760) by ADCC with NK cells. Migration of a $CD25^+$ CD4 Treg population sorted from PBMCs in healthy donors to a CCL22/MDC gradient was abrogated by the pretreatment of PBMCs with an anti-hCCR4 (KM2760) mAb. The inhibition of the proliferative response of CD4 and CD8 T cells stimulated with anti-CD3/CD28-coated beads by $CD25^+CD127^{dim/-}$ CD4 Tregs was abrogated by adding anti-hCCR4 mAb (KM2760) and $CD56^+$ NK cells to the culture. These in vitro findings of efficient elimination of Tregs in a migration assay and in a T cell proliferation assay may give the basis for implementation of clinical trials focusing on depletion of Tregs by administration of anti-hCCR4 mAb to cancer patients with various solid tumors.

In this study, we showed that an anti-hCCR4 mAb (KM2760) had no direct blocking activity on the migration of purified CD4 T cells to the CCL22/MDC gradient by simply adding it to the culture during the assay. There is extensive redundancy in the binding for chemokines to chemokine receptors.[28] It is possible that chemokine receptors other than CCR4 are involved in the migration to the CCL22/MDC gradient under the CCR4 blockade.[29] Or it could simply be due to the lack of blocking activity for CCL22/MDC binding to CCR4.

Recently, Sugiyama et al. showed depletion of activated/effector Tregs and augmentation of T cell responses against the NY-ESO-1 antigen by magnetic bead depletion using a biotin anti-CCR4 mAb (1G1) and also by simply adding a mouse anti-human CCR4 mAb (KM2160) to the culture.[30] In our study, we showed that a defucosylated chimeric KM2760 derived from KM2160 efficiently depleted Tregs by ADCC with NK cells as above. However, with KM2760, no depletion of any Treg subpopulations and no effect on their migration to CCL22/MDC was observed without

adding NK cells. The difference in the direct depletion effect between KM2160 and KM2760 by adding to the culture could be due to experimental systems, especially incubation time (7 days in their study and 4 hrs in ours) or due to loss of depleting activity by chimerization and defucosylation of the antibody, although less likely. This point should be carefully addressed in future studies.

Induction of immune responses by depleting Tregs has been reported previously.[31, 32] In vitro depletion of $CD25^+$ cells induced activation of NY-ESO-1-specific naïve CD4 T cell precursors in stimulation with NY-ESO-1 peptides in PBMCs from healthy donors and from NY-ESO-1-expressing melanoma patients who had no NY-ESO-1 antibodies.[33] We previously showed that depletion of Tregs by in vivo administration of an anti-CD25 mAb (clone PC61) caused rejection of tumors that otherwise grew progressively in murine tumor models.[7] However, the effect of inducing tumor rejection by administration of the mAb was observed only up to day 2 after tumor inoculation. This is probably due to the depletion of the effector T cells which were generated after recognition of the tumor cells and express CD25 on their cell surfaces.[34] There are some reports of clinical trials on the depletion of CD25 Tregs using anti-CD25 or diphtheria toxin-conjugated IL-2 (denileukin diftitox).[35, 36] The results in those studies were controversial: successful depletion of $CD25^+$ cells and augmentation of the tumor immune response in one study[37], but no effect in the others.

We are currently conducting a phase I clinical trial administering humanized anti-hCCR4 mAb (KW-0761) to patients with various solid tumors. Depletion of CCR4-expressing activated/effector Tregs in PBMCs will result in depletion of either CCR4-expressing or non-expressing activated/effector Tregs in the tumor if they migrate from the peripheral blood. On the other hand, the findings that high and low frequencies of CCR4-expressing cells in activated/effector Tregs and resting/naïve Tregs, respectively, in PBMCs may suggest that the CCR4 expression is correlated

with Treg function, and only the CCR4-expressing population represents functional Tregs in TILs, although this remains to be clarified. Our preliminary results show efficient depletion of CCR4-expressing activated/effector Tregs in PBMCs, although those cells in the TILs were not analyzed.

Off-target effects could occur due to anti-CCR4 mAb therapy. CCR4 is expressed on Th2 and Th17 cells other than Tregs, but not on Th1 cells (data not shown). Depletion of these cells may cause impaired antibody and cellular responses against infection. CD8 and monocytes express no CCR4 (our unpublished observation).[30] Studies on ATL/ATLL patients and our preliminary study on solid tumor patients showed that eruption controllable by steroids probably caused by autoimmunity was commonly observed, while infection was rare.[27]

CCR4 expression on tumor cells is controversial. Frequent expression was reported with head and neck cancer[38] and moderate expression was reported with other cancers.[39, 40] In lung cancer, however, IHC analysis of TMA in this study showed that CCR4 expression on tumor cells was observed in only one of 384 specimens. These findings suggest that the ADCC caused by anti-hCCR4 mAb (KW-0761) acts against CCR4-expressing lymphocytes, but not tumor cells, in lung cancer.

Acknowledgments

We thank Kyowa Hakko Kirin for providing the anti-CCR4 (KM2760) mAb for this study and Dr. Junya Fukuoka of Nagasaki University Graduate School, Nagasaki, Japan for help scoring IHC using TMA. We also thank Ms. Junko Mizuuchi for preparation of the manuscript.

References

1. Fridman WH, Pages F, Sautes-Fridman C, et al. The immune contexture in human tumours: impact on clinical outcome. *Nat Rev Cancer* 2012;12:298-306.
2. Wang HY, Lee DA, Peng G, et al. Tumor-specific human CD4+ regulatory T cells and their ligands: implications for immunotherapy. *Immunity* 2004;20:107-118.
3. Bonertz A, Weitz J, Pietsch DH, et al. Antigen-specific Tregs control T cell responses against a limited repertoire of tumor antigens in patients with colorectal carcinoma. *J Clin Invest* 2009;119:3311-3321.
4. Sato E, Olson SH, Ahn J, et al. Intraepithelial CD8+ tumor-infiltrating lymphocytes and a high CD8+/regulatory T cell ratio are associated with favorable prognosis in ovarian cancer. *Proc Natl Acad Sci U S A* 2005;102:18538-18543.
5. Hiraoka N, Onozato K, Kosuge T, et al. Prevalence of FOXP3+ regulatory T cells increases during the progression of pancreatic ductal adenocarcinoma and its premalignant lesions. *Clin Cancer Res* 2006;12:5423-5434.
6. Jandus C, Bioley G, Speiser DE, et al. Selective accumulation of differentiated FOXP3(+) CD4 (+) T cells in metastatic tumor lesions from melanoma patients compared to peripheral blood. *Cancer Immunol Immunother* 2008;57:1795-1805.
7. Onizuka S, Tawara I, Shimizu J, et al. Tumor rejection by in vivo administration of anti-CD25 (interleukin-2 receptor alpha) monoclonal antibody. *Cancer Res* 1999;59:3128-3133.
8. Miyara M, Sakaguchi S. Human FoxP3(+)CD4(+) regulatory T cells: their knowns and unknowns. *Immunol Cell Biol* 2011;89:346-351.
9. Yamagiwa S, Gray JD, Hashimoto S, et al. A role for TGF-beta in the generation and expansion of CD4+CD25+ regulatory T cells from human peripheral blood. *J Immunol* 2001;166:7282-7289.
10. Bromley SK, Mempel TR, Luster AD. Orchestrating the orchestrators: chemokines in control of T cell traffic. *Nat Immunol* 2008;9:970-980.
11. Campbell DJ, Koch MA. Phenotypical and functional specialization of FOXP3+ regulatory T cells. *Nat Rev Immunol* 2011;11:119-130.
12. Imai T, Baba M, Nishimura M, et al. The T cell-directed CC chemokine TARC is a highly specific biological ligand for CC chemokine receptor 4. *J Biol Chem* 1997;272:15036-15042.
13. Imai T, Chantry D, Raport CJ, et al. Macrophage-derived chemokine is a functional ligand for the CC chemokine receptor 4. *J Biol Chem* 1998;273:1764-1768.
14. Hori S, Nomura T, Sakaguchi S. Control of regulatory T cell development by the transcription factor Foxp3. *Science* 2003;299:1057-1061.
15. Miyara M, Yoshioka Y, Kitoh A, et al. Functional delineation and differentiation

dynamics of human CD4+ T cells expressing the FoxP3 transcription factor. *Immunity* 2009;30:899-911.
16. Fukuoka J, Fujii T, Shih JH, et al. Chromatin remodeling factors and BRM/BRG1 expression as prognostic indicators in non-small cell lung cancer. *Clin Cancer Res* 2004;10:4314-4324.
17. Kanegasaki S, Nomura Y, Nitta N, et al. A novel optical assay system for the quantitative measurement of chemotaxis. *J Immunol Methods* 2003;282:1-11.
18. Yamauchi A, Degawa-Yamauchi M, Kuribayashi F, et al. Systematic single cell analysis of migration and morphological changes of human neutrophils over stimulus concentration gradients. *J Immunol Methods* 2014;404:59-70.
19. Niwa R, Shoji-Hosaka E, Sakurada M, et al. Defucosylated chimeric anti-CC chemokine receptor 4 IgG1 with enhanced antibody-dependent cellular cytotoxicity shows potent therapeutic activity to T-cell leukemia and lymphoma. *Cancer Res* 2004;64:2127-2133.
20. Nishikawa H, Sakaguchi S. Regulatory T cells in cancer immunotherapy. *Curr Opin Immunol* 2014;27C:1-7.
21. Zou W, Restifo NP. T(H)17 cells in tumour immunity and immunotherapy. *Nat Rev Immunol* 2010;10:248-256.
22. Chen X, Wan J, Liu J, et al. Increased IL-17-producing cells correlate with poor survival and lymphangiogenesis in NSCLC patients. *Lung Cancer* 2010;69:348-354.
23. Chang SH, Mirabolfathinejad SG, Katta H, et al. T helper 17 cells play a critical pathogenic role in lung cancer. *Proc Natl Acad Sci U S A* 2014.
24. Mariani M, Lang R, Binda E, et al. Dominance of CCL22 over CCL17 in induction of chemokine receptor CCR4 desensitization and internalization on human Th2 cells. *Eur J Immunol* 2004;34:231-240.
25. Niwa R. Defucosylated Chimeric Anti-CC Chemokine Receptor 4 IgG1 with Enhanced Antibody-Dependent Cellular Cytotoxicity Shows Potent Therapeutic Activity to T-Cell Leukemia and Lymphoma. *Cancer Res* 2004;64:2127-2133.
26. Ishida T, Ueda R. Antibody therapy for Adult T-cell leukemia-lymphoma. *Int J Hematol* 2011;94:443-452.
27. Yamamoto K, Utsunomiya A, Tobinai K, et al. Phase I study of KW-0761, a defucosylated humanized anti-CCR4 antibody, in relapsed patients with adult T-cell leukemia-lymphoma and peripheral T-cell lymphoma. *J Clin Oncol* 2010;28:1591-1598.
28. Horuk R. Chemokine receptor antagonists: overcoming developmental hurdles. *Nat Rev Drug Discov* 2009;8:23-33.
29. Schall TJ, Proudfoot AE. Overcoming hurdles in developing successful drugs targeting chemokine receptors. *Nat Rev Immunol* 2011;11:355-363.
30. Sugiyama D, Nishikawa H, Maeda Y, et al. Anti-CCR4 mAb selectively depletes effector-type FoxP3+CD4+ regulatory T cells, evoking antitumor immune responses in

humans. *Proc Natl Acad Sci U S A* 2013;110:17945-17950.
31. Klages K, Mayer CT, Lahl K, et al. Selective depletion of Foxp3+ regulatory T cells improves effective therapeutic vaccination against established melanoma. *Cancer Res* 2010;70:7788-7799.
32. Teng MW, Ngiow SF, von Scheidt B, et al. Conditional regulatory T-cell depletion releases adaptive immunity preventing carcinogenesis and suppressing established tumor growth. *Cancer Res* 2010;70:7800-7809.
33. Nishikawa H, Jager E, Ritter G, et al. CD4+ CD25+ regulatory T cells control the induction of antigen-specific CD4+ helper T cell responses in cancer patients. *Blood* 2005;106:1008-1011.
34. Ko K, Yamazaki S, Nakamura K, et al. Treatment of advanced tumors with agonistic anti-GITR mAb and its effects on tumor-infiltrating Foxp3+CD25+CD4+ regulatory T cells. *J Exp Med* 2005;202:885-891.
35. Jacobs JF, Punt CJ, Lesterhuis WJ, et al. Dendritic cell vaccination in combination with anti-CD25 monoclonal antibody treatment: a phase I/II study in metastatic melanoma patients. *Clin Cancer Res* 2010;16:5067-5078.
36. Attia P, Maker AV, Haworth LR, et al. Inability of a fusion protein of IL-2 and diphtheria toxin (Denileukin Diftitox, DAB389IL-2, ONTAK) to eliminate regulatory T lymphocytes in patients with melanoma. *J Immunother* 2005;28:582-592.
37. Rech AJ, Mick R, Martin S, et al. CD25 blockade depletes and selectively reprograms regulatory T cells in concert with immunotherapy in cancer patients. *Sci Transl Med* 2012;4:134ra162.
38. Tsujikawa T, Yaguchi T, Ohmura G, et al. Autocrine and paracrine loops between cancer cells and macrophages promote lymph node metastasis via CCR4/CCL22 in head and neck squamous cell carcinoma. *Int J Cancer* 2013;132:2755-2766.
39. Yang YM, Feng AL, Zhou CJ, et al. Aberrant expression of chemokine receptor CCR4 in human gastric cancer contributes to tumor-induced immunosuppression. *Cancer Sci* 2011;102:1264-1271.
40. Nakamura ES, Koizumi K, Kobayashi M, et al. RANKL-induced CCL22/macrophage-derived chemokine produced from osteoclasts potentially promotes the bone metastasis of lung cancer expressing its receptor CCR4. *Clin Exp Metastasis* 2006;23:9-18.

Figure Legends

Figure 1. Analysis of subpopulations of $Foxp3^+$ CD4 T cells and expression of CCR4 on those cells in PBMCs and TILs from lung cancer patients. A, classification of $Foxp3^+$ CD4 T cells as $CD45RA^+$ $Foxp3^{lo}$ resting/naïve Tregs (Fr 1), $CD45RA^-$ $Foxp3^{hi}$ activated/effector Tregs (Fr 2) and $CD45RA^-$ $Foxp3^{lo}$ non Tregs (Fr 3). B, representative dot plots showing subpopulations of $Foxp3^+$ CD4 T cells in PBMCs and TILs and histograms showing the CCR4 expression on those cells using anti-hCCR4 mAb (1G1) and the isotype-mached control Ab (gray). Figures indicate % positive cells. C, ratios of resting/naïve and activated/effector Tregs, and non Tregs in CD4 T cells (left panel) and CCR4 expression on those cells (right panel) in PBMCs and TILs from 20 lung cancer patients. Horizontal bar, mean value. Statistical analysis was done by the Mann-Whitney U-test (****, $p < 0.0001$). Each dot indicates a single patient.

Figure 2. Analysis of CCR4, CCL17/TARC and CCL22/MDC expressing cells in lung cancer by IHC using a tissue microarray (TMA). A, staining score was determined by a sum of scores of distribution (D) and intensity (I) (see Materials and Methods). Representative intensity (I) scoring with density (D) score 1 for CCR4 and CCL22 are shown. Two TMA spots were examined in each sample and the mean score was calculated for the definitive score. A definitive score exceeding 2 ($\geq$ 2.5) was considered positive. Scale bar denotes 100 μm for low magnification and 50 μm for high magnification (inset). B, representative staining of TMA with CCR4 (score 3), CCL17/TARC (score 0) and CCL22/MDC (score 3) and the number of positive samples for stroma-infiltrating cells and tumor cells in the total of 384 samples are shown. HE, hematoxylin/eosin. Scale bar denotes 100 μm.

Figure 3. A, IHC staining of TMA with anti-CCR4, anti-CD4 and anti-Foxp3 in lung cancer tissue. In double staining of CCR4 and CD4, CCR4 is stained brown and CD4 is stained red. Arrows indicate double stained cells. ATL is a positive control. Staining of CCR4 and Foxp3 are done on serial sections. Arrows show the cells stained with either mAb. Scale bar denotes 100 μm. B, IHC staining of serial sections with anti-CCL22 and anti-CD163. Arrows show the cells stained with either mAb. C, Correlation of CCR4 with CCL22 score. $CCL22^-$ (score 0 – 2): n=267, $CCL22^+$ (score ≥ 2.5): n=117. CCR4 score is the mean value with the error bar showing 95%CI. Statistical analysis was done by the Mann-Whitney U-test.

Figure 4. Efficient migration of a $CCR4^+$ $CD25^+$ CD4 T cell population in PBMCs to the CCL22/MDC gradient and elimination of migrating cells by adding an anti-CCR4 (KM2760) mAb to the culture. A, migration of $CD25^+$ CD4 T cells ($CD25^+KM^-$ and $CD25^+KM^+$) sorted from PBMCs which were left untreated or treated with anti-hCCR4 mAb (KM2760), respectively, using FACS Aria to the CCL22/MDC gradient was investigated using EZ-TAXIScan apparatus. $CCR4^+$ CD4 T cells and the $CCR4^-$ CD4 T cells sorted from anti-hCCR4 (1G1) mAb (without ADCC activity) and anti-hCD4 mAb-treated PBMCs were used as positive and negative controls, respectively, for migration. The results are the mean ± SD of duplicates. B, the % migrating cells to CCL22/MDC counted at 30 min in the assay. The results are the mean ± SD of three individuals. Statistical analysis was done by Welch's t-test (** $p < 0.01$, **** $p < 0.0001$). In C, blocking of Treg migration by an anti-hCCR4 (KM2760) mAb was investigated. Purified CD4 T cells ($1x10^5$) were placed in the upper chambers and CCL22 (100 ng/ml) was placed in the lower chambers of Transwell plates. A different amount of anti-hCCR4 (KM2760) mAb was present in the upper and lower chambers during the

migration assay. After incubation for 4 hrs, all cells in the lower chambers were collected and the number of cells was counted with a FACS Canto II. FACS dot plots showed subpopulations of Foxp3^{+} CD4 T cells (top). Numbers in the dot plot panel denote % of resting/naïve Tregs, non Tregs and activated/effector Tregs in the migrated Foxp3+ CD4 T cells from top to bottom. Migration of non Tregs and activated/effector Tregs to CCL22/MDC was observed, but no blocking of migration by addition of KM2760 was observed. Numbers of migrating CD4 T cells (bottom left) and activated/effector Tregs (bottom right) are shown. The results are the mean ± SD of triplicate experiments. Statistical analysis was done by the Welch's t-test for two groups and by ANOVA for multiple groups (** $p < 0.01$). No blocking of migration was observed.

Figure 5.

Inhibition of CD3/CD28-mediated proliferative response of CD4 and CD8 T cells by CD25^{+} Tregs and abrogation of inhibition by the treatment of Tregs with anti-hCCR4 mAb (KM2760). A, schema of the experimental protocol. CD127$^{dim/-}$ CD4 T cells were indirectly purified from the PBMCs of healthy donors using biotin-conjugated antibodies against CD8, CD19, CD123 and CD127 with anti-biotin antibody-coated magnetic beads. CD25^{+} CD127$^{dim/-}$ CD4 Tregs were then purified and CD25^{-} CD127$^{dim/-}$ CD4 T cells were used as control non Tregs. CD56^{+} NK cells, and CD4 and CD8 T cells were purified from PBMCs also using antibody-coated magnetic beads. Tregs (1×10^4) and CD56^{+} NK cells (1×10^4) were incubated overnight with or without anti-hCCR4 mAb (KM2760) at a concentration of 10 μg/ml in 96-well culture plates. After washing the cells in the plates, anti-CD3/CD28 beads were added. The CFSE-labeled responder CD4 and CD8 T cells were then added and proliferation was determined after 5-6 days. In B, representative results of three independent

experiments are shown. Dot plots and histograms of CFSE-labeled CD4 and CD8 T cells after stimulation with anti-CD3/CD28, and inhibition of proliferation by Tregs and its abrogation by anti-hCCR4 mAb (KM2760) treatment are shown. C, layered presentation of the experiment shown in B. D, the results in B are shown as the mean ± SD of triplicate experiments. Statistical analysis was done by Welch's t-test (** $p < 0.01$, *** $p < 0.001$).

Characteristics	Patients	
Age, years		
Median	76.5	
Range	58-85	
□65	16	80 (%)
Sex		
Male	17	85
Female	3	15
BMI (kg/m^2)	22.6 ± 2.6	
Smoking status		
Never	4	20
Former	13	65
Current	3	15
Pack-years	46.8 ± 37.8	
FEV_1 / FVC (%)	68.0 ± 10.3	
FEV_1 % predicted	106.4 ± 17.1	
Pathologic stage		
□A	6	30
□B	4	20
□A	6	30
□B	0	0
□A	4	20
Histology		
Adenocarcinoma	12	60
Squamous cell carcinoma	5	25
Large cell carcinoma	2	10

Adenosquamous cell carcinoma	1	5	

Table 1. Patient characteristics (n=20)

Fig. 1

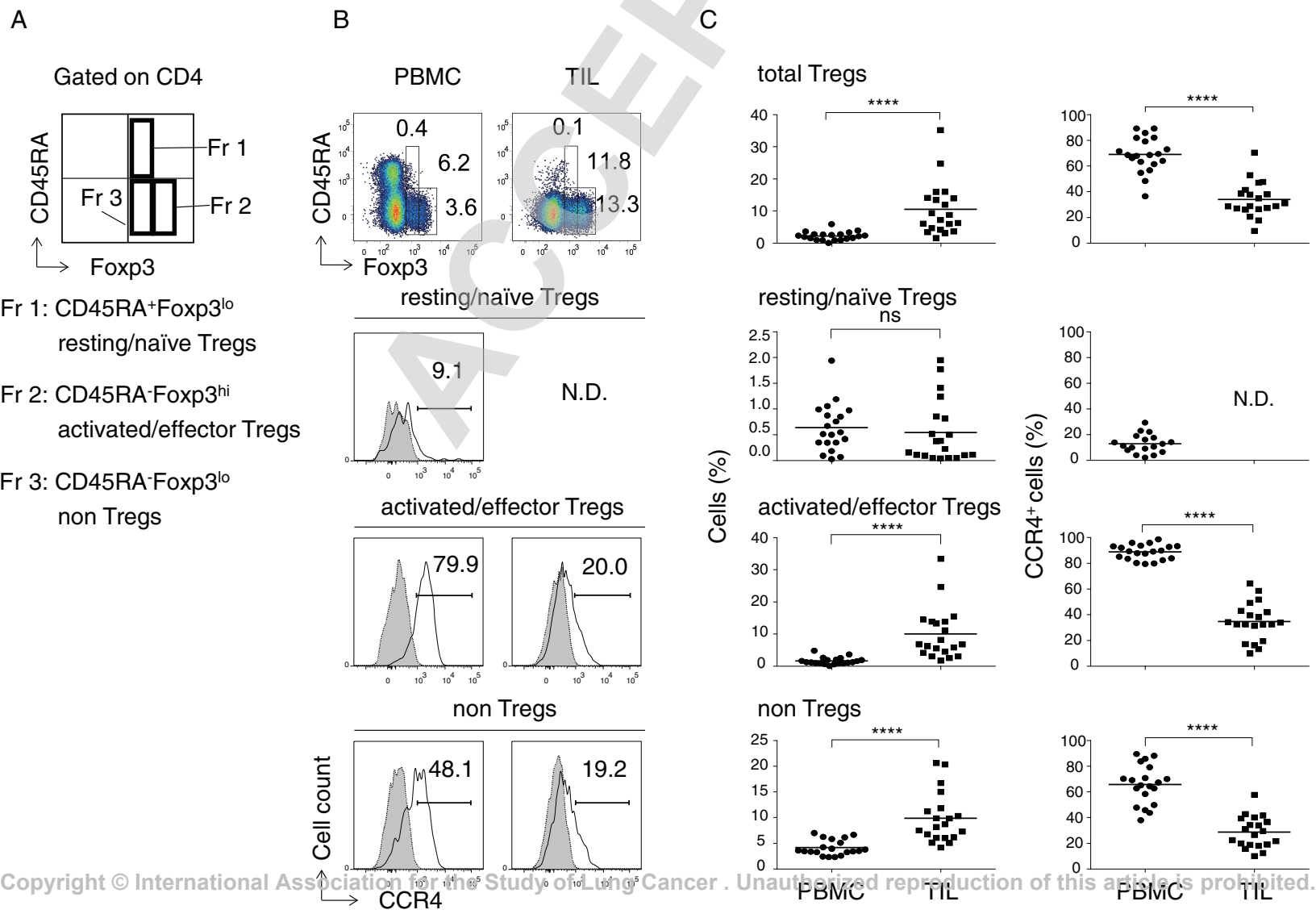

Fig. 2

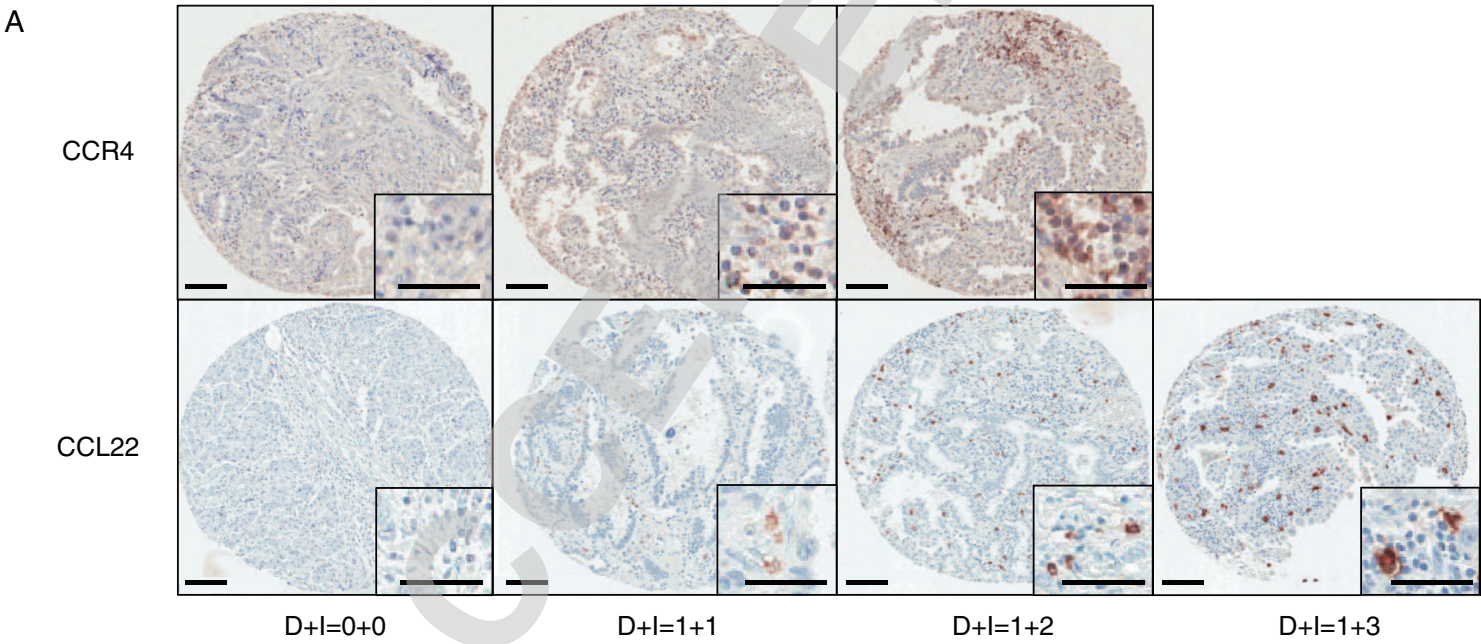

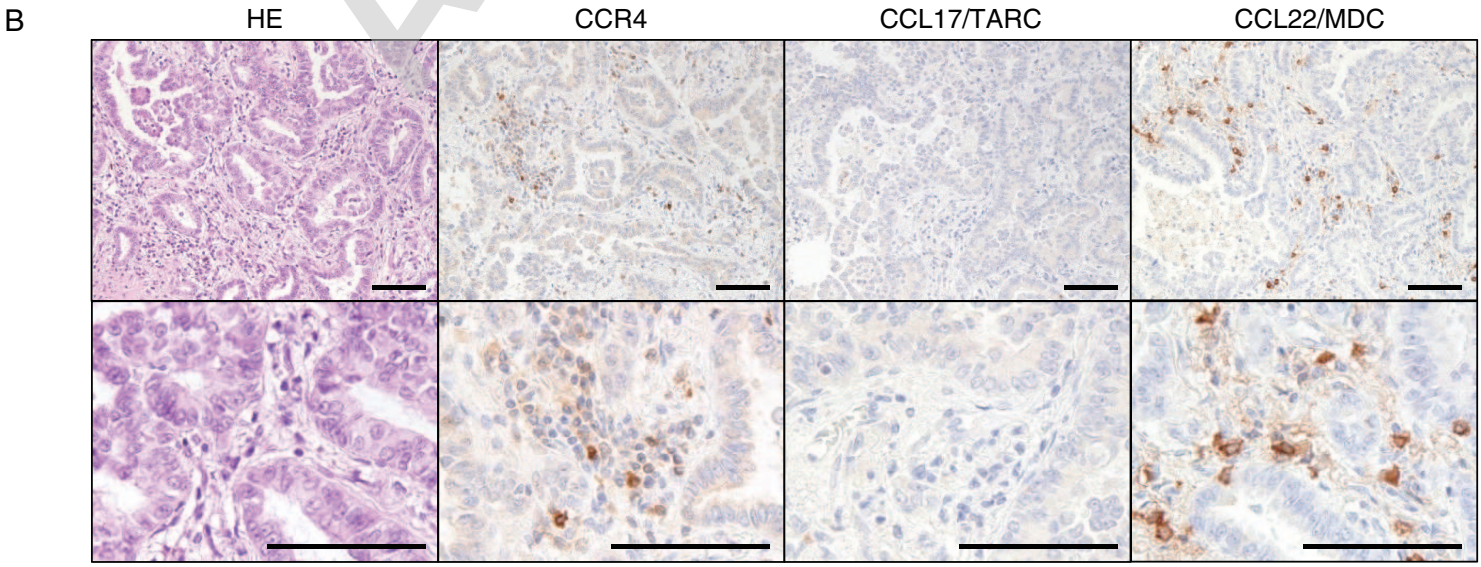

Stroma	78/384 (20.3%)	5/384 (1.3%)	117/384 (30.5%)
Tumor	1/384 (0.3%)	2/384 (0.5%)	0/384 (0%)

Fig. 3

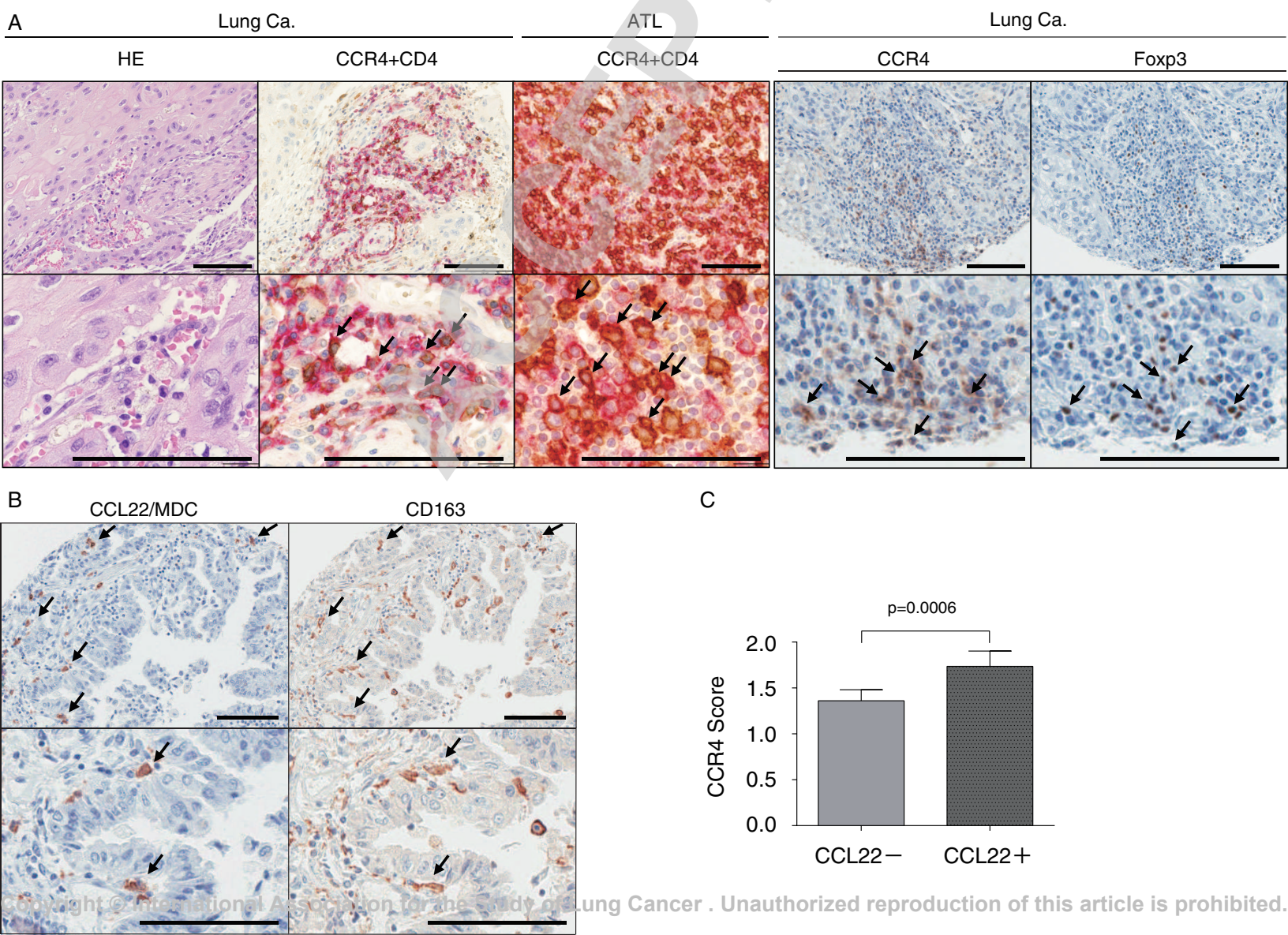

Fig. 4

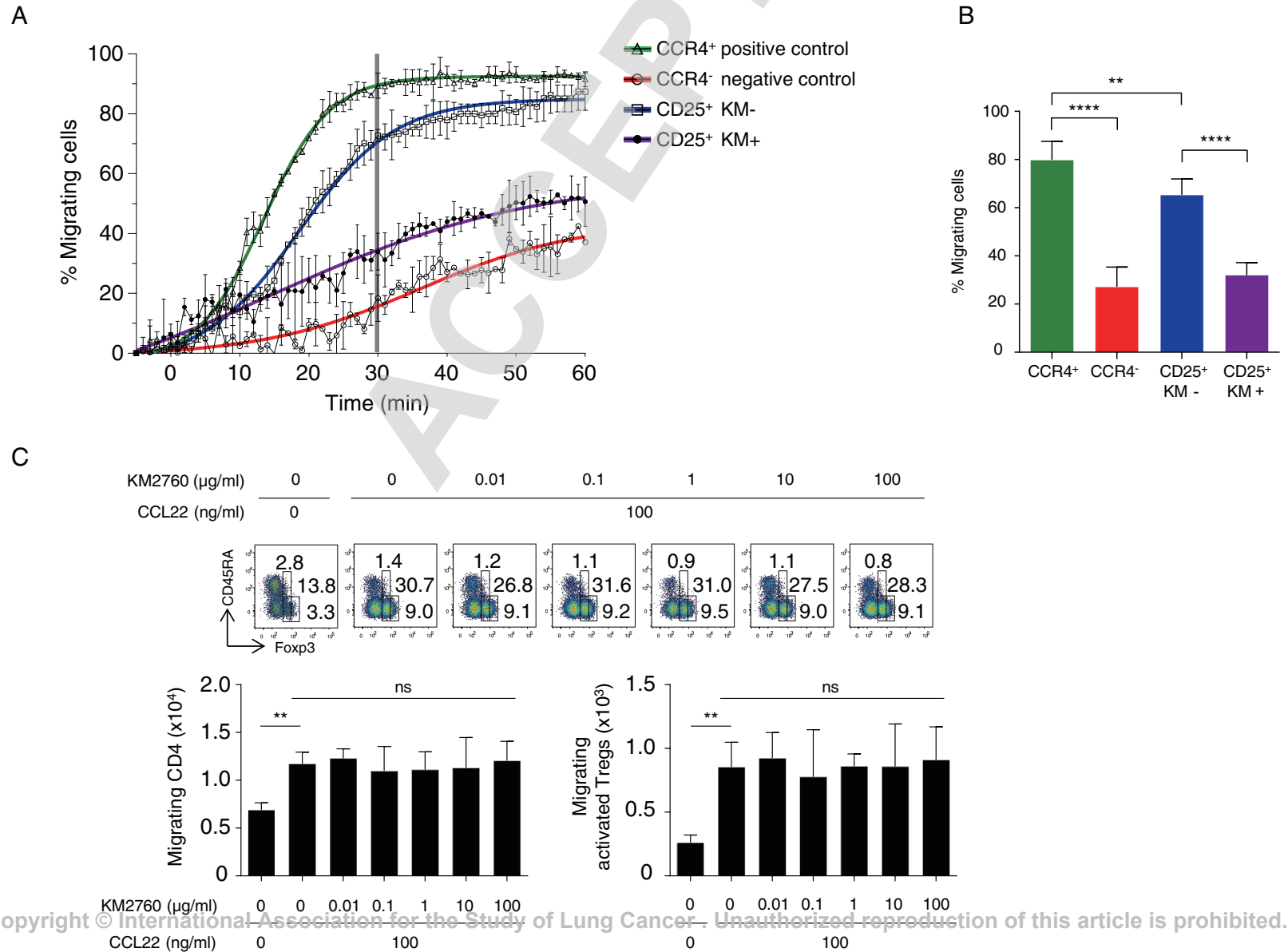

Figure5

Fig. 5